The Compact Muon Solenoid Experiment

CMS Note

Mailing address: CMS CERN, CH-1211 GENEVA 23, Switzerland

June 12, 2006

Measurement of open beauty production at LHC with CMS

Valery P. Andreev, David B. Cline, Stanislaw Otwinowski

University of California Los Angeles,
Department of Physics and Astronomy,
405 Hilgard Avenue,
Los Angeles,
CA 90024-1547, USA

Abstract

At the LHC new opportunities to improve our understanding of the physics of the b quark will become available because of the high statistics data samples and the high center-of-mass energy that the new accelerator will provide. The CMS collaboration will measure the cross section for inclusive b production in proton-proton collisions at $\sqrt{s} = 14$ TeV. A study has been performed to investigate methods of identifying b jets (b "tagging") in an inclusive sample of events containing jets and at least one muon. We present the CMS capability to measure the inclusive b production cross section as a function of B-hadron transverse momentum and pseudorapidity.

1 Introduction

Bottom flavored hadrons can be used for CP-violation measurement, for QCD tests, for B decays studies, and are an important source of background for several processes of interest. B tagging is a crucial ingredient of the new physics (Higgs, SUSY, ...) searches at the LHC. At the LHC new opportunities to improve our understanding of the physics of b quarks will become available because of the high statistics data samples and the high center-of-mass energy provided. The present status of the production phenomenology at hadron colliders is the following. On one side, the shape of transverse momentum and angular distributions as well as the azimuthal angular correlations are reasonably well explained by perturbative QCD. On the other side, however, the observed cross-sections at the Tevatron (Run I) are larger than QCD predictions [1, 2, 3, 4, 5, 6, 7, 8]. Similar effects are observed in $\gamma\mathrm{p}$ collisions at HERA [9, 10, 11, 12, 13, 14, 15] and in $\gamma\gamma$ interactions at LEP [16, 17]. The Tevatron Run II data have confirmed and extended Run I heavy flavor data. In the meantime, an agreement between experiment and theory has improved due to the evolution of latter (more precise parton density functions and proper fragmentation effects estimate) [18, 19, 20, 21, 22, 23]. The agreement is not complete and the improvement of the phenomenological description requires new experimental input.

B production will be one of the most copious sources of hadrons at LHC. We performed a study on Monte Carlo events generated with PYTHIA [24] to investigate methods in CMS of identifying b jets (b "tagging") in an inclusive sample of events containing jets and at least one muon. We present the capability to measure the inclusive b quark production cross section as a function of the B-hadron transverse momentum and pseudorapidity. An important result of our study is an estimate for the highest B-hadron p_{T} range for a cross section measurement reachable at LHC.

Since the tagging of a b inside the jet is almost independent of the details of the $b \to B$ fragmentation, measuring the rate of b jets is a direct measurement of the b production rate with a small fragmentation systematics [22, 23]. In addition, large logarithms due to hard collinear gluons are avoided when all fragmentation modes are integrated. This reduces model dependence (improves the perturbative accuracy) when comparing experimental data with theory.

Three mechanisms contribute to the beauty production at hadron colliders: gluon-gluon fusion and $\mathrm{q\overline{q}}$ annihilation (flavor creation in hard QCD scattering), flavor excitation (semi-hard process) and gluon splitting (soft process). It is important to measure the B-hadron p_{T} spectra within large range to be able to disentangle the contributions of those mechanisms. At the Tevatron inclusive B spectra have been measured up to $100\ \mathrm{GeV}/c$ by D0 and up to $200\ \mathrm{GeV}/c$ by CDF.

2 Analysis

2.1 Event generation

Samples of QCD jets generated with PYTHIA were used in the analysis. Jets in those samples cover the full geometrical acceptance in pseudorapidity of the tracking detector, $|\eta| < 2.4$. For the studies described in this Note the iterative cone jet reconstruction algorithm [25] with a cone size $\Delta R = \sqrt{\Delta\phi^2 + \Delta\eta^2} < 0.5$ was used. The jet clustering uses as an input the energy deposition in the towers from the electromagnetic and hadronic calorimeters applying a variable noise subtraction. A calibration as deduced from the Monte Carlo simulation has been applied to correct the raw jet energy [26, 27]. The jet response was calibrated up to 4500 GeV [26]. In the CDF experiment, it has been shown that total energy of particles in various cones in the vicinity of a parton is well simulated by PYTHIA, enabling the parton energy scale to be corrected to the particle-level jet energy scale via Monte Carlo simulation derived correction factors (p_{T}-jet / p_{T}-parton). Those corrections are less than 5 % for jets with $E_{\mathrm{T}} > 50\ \mathrm{GeV}/c$ [28]. As shown in reference [28] CMS has developed a data-driven calibration strategy that will be used in the real analysis. This has been shown to be feasible using di-jets events up to about 1.5 TeV.

The PYTHIA generator $\mathrm{b\overline{b}}$ production includes diagrams from each production mechanism mentioned in the introduction. Flavor creation refers to the lowest-order, two-to-two QCD $\mathrm{b\overline{b}}$ production diagrams. Flavor excitation corresponds to diagrams where a $\mathrm{b\overline{b}}$ pair from the quark sea of the proton is excited into the final state due to one of the b quarks undergoes a hard QCD interaction with a parton from the other proton. Gluon splitting refers to the processes in which the $\mathrm{b\overline{b}}$ pair arises from a $g \to \mathrm{b\overline{b}}$ splitting in the initial or final state. Neither of the quarks from $\mathrm{b\overline{b}}$ pair participate in the hard QCD scattering in this case. PYTHIA uses the parton shower model to estimate the effects of higher-order corrections. The exact matrix elements for all parton-parton two-to-two scatterings are combined with initial- and final-state radiation using a probabilistic approach.

A study of CMS capability to measure the inclusive b production is based on a full detector simulation. The generated events are passed through the GEANT4 [29] simulation of CMS. Pile-up corresponding to the low luminosity LHC run ($\mathcal{L} = 2 \times 10^{33}\ \mathrm{cm}^{-2}\,\mathrm{s}^{-1}$) is also generated and superimposed to the original event.

The CMS reconstruction program ORCA [30] was applied in the analysis. About 4 millions QCD containing both B-hadrons (signal) as well as other flavour (background) events were processed, mainly with high transverse momentum of the partons ($p_{\mathrm{T}} > 50\ \mathrm{GeV}/c$). The events were processed on the LHC Computing Grid using the ASAP (ARDA Support for cms Analysis Process) job submission and monitoring tool [31].

2.2 Event selection

The measurement of the differential cross sections is studied for B-hadrons produced in the fiducial volume of

$$p_{\mathrm{T}} > 50\ \mathrm{GeV}/c$$

$$|\eta| < 2.4$$

First, the events are required to pass the Level-1 (L1) trigger [32] selection for the single muon trigger stream which accepts events with muons having $p_{\mathrm{T}} > 14\ \mathrm{GeV}/c$. For the High Level Trigger (HLT) selection we require the single muon trigger to be fired by non-isolated muons with $p_{\mathrm{T}} > 19\ \mathrm{GeV}/c$. Those thresholds correspond to the latest CMS trigger tables. At HLT selection we require the "muon + b-jet" trigger, fired by non-isolated muons with $p_{\mathrm{T}} > 19\ \mathrm{GeV}/c$ and by jets with $E_{\mathrm{T}} > 50\ \mathrm{GeV}/c, |\eta| < 2.4$ compatible with b tagging. Muon threshold corresponds to the standard HLT single muon trigger without muon isolation requirement. Then it is combined into cross-channel trigger with b-jets trigger. Details on b-jets trigger are in [33]. The proposed muon plus b-jet cross-channel trigger has 4.3 Hz rate for the signal and 6.1 Hz total event rate. The trigger rate corresponds to the low luminosity LHC run at $\mathcal{L} = 2 \times 10^{33}\ \mathrm{cm}^{-2}\,\mathrm{s}^{-1}$. The trigger rate can be tuned with thresholds selection. In the CMS L1 trigger menu there is "muon + jet" stream. At the time of the writing of this Note, it has been considered with L1 muon and jet thresholds of $p_{\mathrm{T}} > 10\ \mathrm{GeV}/c$ and $E_{\mathrm{T}} > 60\ \mathrm{GeV}/c$, respectively. We verified that more than 95 % of selected events would be also accepted by such trigger. The high p_{T} part of the spectrum is also effectively selected by single jet trigger, the pre-scaled central single jet trigger with pre-scaling at 20 GeV/c, 60 GeV/c, 120 GeV/c and 250 GeV/c E_{T} thresholds, and unscaled single jet trigger at $E_{\mathrm{T}} > 400\ \mathrm{GeV}/c$ [34].

The efficiencies for the L1 and HLT triggers are shown in Figure 1 and Figure 2, respectively. The efficiencies are presented as function of B-hadron transverse momentum and pseudorapidity for events in which the most energetic B-hadron is inside of the phase space defined above. The trigger efficiency is flat as a function of the B-hadron pseudorapidity (the L1 trigger acceptance is limited to $|\eta| < 2.1$), while being a rising function of the B-particle transverse momentum. The average L1 trigger efficiency corresponds to the expected value of branching fractions sum for the semileptonic b quark and the cascade c quark decays, about 19 % [35].

The offline selection requires a b tagged jet to be present in the event. B tagging is based on inclusive secondary vertex reconstruction in jets [36]. The B-tagging algorithm combines several topological and kinematic secondary vertex related variables into a single tagging variable to discriminate between jets originating from b quarks and those from light quarks and gluons. The relatively large lifetime of B-hadrons ($\sim$ 1.5 ps) leads to secondary vertices displaced from the primary event vertex. B-hadrons have a large mass, large multiplicity of charged particles in the final state and B carries a large fraction of the jet energy due to the hard b fragmentation function.

In order to measure the differential cross sections for inclusive B-particle production as a function of its transverse momentum p_{T} and pseudorapidity η, $d\sigma/dp_{\mathrm{T}}$ and $d\sigma/d|\eta|$, we select as reconstructed B-particle candidate the most energetic b tagged jet. Figure 3 shows the reconstructed (dots) p_{T} and pseudorapidity η spectra of the most energetic b tagged jet versus p_{T} and pseudorapidity of the most energetic generated B-particle (histograms). Good correspondence between the generated B-particle and the reconstructed b-tagged jet is observed. The corresponding p_{T} and pseudorapidity resolutions are shown in the Figure 4 for B-particles with $p_{\mathrm{T}} > 170\ \mathrm{GeV}/c$. The resolutions are 13 % (relative resolution) and 0.04 for p_{T} and pseudorapidity, respectively.

The efficiency of the b tagging in jets is shown in Figure 5 as function of the B-particle transverse momentum and pseudorapidity. The efficiency decreases with increasing transverse momentum, while being rather flat as function of pseudorapidity. The slow degradation for larger transverse momenta is caused by the worsening of the tracking resolution with increasing p_{T}, an increased track multiplicity from fragmentation and more difficult pattern recognition in dense jets. The average b tagging efficiency is 65 % in the barrel region, while the efficiency is about 10 % less for the endcap region.

To measure the cross section one needs to know the number of selected events, the integrated luminosity, the event sample purity (signal fraction) and the signal efficiency. The signal fraction can be determined from the simulation. In order to rely less on the absolute value prediction for the background one can extract the signal fraction using the prediction of the signal and background shapes for some sensitive variables. A fit of the data distribution by the simulated shapes for the signal and background is performed with a lepton tag by applying inclusive muons.

2.3 Muon tag

Muons are reconstructed in the muon chambers, matched to the tracker information and their trajectory is refitted using both subdetectors information [28]. Each reconstructed muon is associated to the most energetic b tagged jet. The muon must be closer to this b tagged jet than to any other jet in the event. If no muon is found or if the muon is not associated to the b tagged jet the event is discarded.

Figure 6 shows the angular distance between the tagged muon and the b tagged jet ($\cos\theta_{\mu-\mathrm{Bjet}}$) as well as the distance to the second closest jet. In most cases the tagged muon is inside the b jet. The muon is relatively easy to identify inside jets as muon reaches the muon chambers after a small energy deposition in the calorimeters. The same figure shows also the tagged muon momentum and its transverse momentum spectra.

In Figure 7 the distributions of the number of jets, number of muons and the number of b tagged jets in the fiducial volume for the same data sample are presented.

The efficiency of the muon association with b tagged jet is shown in Figure 8. The average efficiency of associating the muon with the b tagged jet is 75 %.

2.4 Results

The transverse momentum of the muon with respect to the b-jet axis effectively discriminates b events from the background. Figure 9 shows the distributions of the muon p_{T} with respect to the closest jet from three sources: beauty events, charm events and light quark events. The p_{T} spectra are very different and are exploited to fit of the selected events to determine the fractions of the muon sources in the sample.

Figure 10 shows an example of the fit of muon p_{T} with respect to the closest jet distribution by the expected shapes for the muons from b, charm and light quark events. The normalization of the three contributions are left as free parameters in the fit. The events in this plot are from a sample of QCD events generated with the PYTHIA "p_{T}-hat" parameter in the range $120 < \hat{p_{\mathrm{T}}} < 170$ GeV/c. Another example of the fit for the sample of the QCD events with "p_{T}-hat" parameter in the range $230 < \hat{p_{\mathrm{T}}} < 300$ GeV/c is shown in Figure 11. The shapes of the distributions in both fits were fixed using an independent QCD sample generated with $170 < \hat{p_{\mathrm{T}}} < 230$ GeV/c. The generated QCD events of all samples were also combined into one sample by normalizing to the same integrated luminosity (10 fb^{-1}) and fitted. Figure 12 shows the result of this fit. We combined the "p_{T}-hat" samples starting from $\hat{p_{\mathrm{T}}} > 120$ GeV/c to avoid large fluctuations in small Monte Carlo statistics of the lower "p_{T}-hat" generated range. The fit results as well as the Monte Carlo input are quoted in Table 1. The event fractions are well reproduced within statistical errors. In the actual experiment the shapes will be verified using data at different selection stages. Also the light-quark background shape will be derived from the data itself by applying an anti-tag selection (b-suppressed event sample).

In Table 2 the b purity, $\mathrm{c\overline{c}}$ and light quark event fractions for the different QCD samples are shown. The b purity changes from about 70 % down to 55 % with transition from low p_{T} events to the high transverse momentum events while being only about 6 % in the initial Monte Carlo sample (before the event selection). The expected number of $\mathrm{b\overline{b}}$ events after event selection is quoted for 10 fb^{-1} integrated luminosity. For the phase space of $p_{\mathrm{T}} > 50$ GeV/c and $|\eta| < 2.4$ the event selection will allow b event statistics of about 16 million events. Our estimate for the B-hadron p_{T} range reachable at LHC with CMS detector is 1.5 TeV/c.

The background contribution from $t\overline{t}$ events has been estimated from a sample of one million simulated events including all decay modes. The corresponding cross section is equal to 500 pb. The total number of $t\overline{t}$ events passing the selection amounts to 104 thousand events for 10 fb^{-1} integrated luminosity corresponding on average to less than 1 % background contribution. The $t\overline{t}$ background becomes more pronounced for the high p_{T} part of the inclusive B spectrum. In the region $p_{\mathrm{T}} > 500$ GeV/c it amounts to 2.4 %.

The total event selection efficiency is about 5 %. By correcting for the semi-leptonic branching ratio of b quarks and c quarks it amounts to about 25 % on average. It turns out that the total efficiency is almost independent of

transverse momentum and angle of the B-particle. Therefore the measurement of the differential cross section is less affected by systematic uncertainties due to bin-by-bin efficiency corrections.

2.5 Systematics Uncertainties

Several potential sources for systematic uncertainties are considered and their impact on the observed cross section is detailed in Table 3. The largest uncertainty arises from the 3 % error on the jet energy scale which leads to a cross section error of 12 % at $E_{\mathrm{T}} > 50$ GeV/c. It drops down to 4 % for the highest p_{T}. Other important uncertainties arise from the event-selection procedure and the Monte Carlo modeling of the detector response, including the lepton identification and the detector resolution on the energy and angular variables which identify the fiducial volume. The effect of these systematic uncertainties is estimated by varying the corresponding cuts and repeating the fits for the newly selected event samples. It results in an uncertainty of 6 %. The expected b-tag systematics for 10 fb^{-1} integrated luminosity is 5 % [28]. The luminosity uncertainty is also 5 % [28].

The trigger efficiency will be determined from the data themselves using a set of independent triggers. Its uncertainty varies with jet p_{T}. We estimate this uncertainty from Monte Carlo studies to change from negligible to 3.0 % at the highest p_{T}. The experimental uncertainties on the semi-leptonic branching ratio of b quarks [35] is also propagated to the measurement. The impact of the detector misalignment on the CMS b tagging performance has been investigated in [36]. The effect has been found to be small (2 %). Muon detection efficiency can be determined with better than 1 % precision [28]. The $t\bar{t}$ background subtraction uncertainty is conservatively taken as absolute value of the $t\bar{t}$ contribution to the considered phase space.

A large contribution is expected from the fragmentation modeling. We estimate the magnitude of the effect from the DO b-jet production measurement at Tevatron [8]. This uncertainty propagates to the cross section as a 9 % effect independent of jet E_{T}.

The estimated statistical, systematic and total uncertainty as function of the b tagged jet transverse momentum with respect to the beam line is shown in Figure 13.

3 Conclusion

The event selection for inclusive b production measurement at CMS will allow to study b production mechanisms on an event sample of 16 million b events for 10 fb^{-1} integrated luminosity. The b purity of the selected events vary as function of transverse momentum in the range from 70 % to 55 %. Our estimate shows that with the CMS detector we can reach 1.5 TeV/c as the highest measured transverse momentum of B hadrons. The results are preliminary, the improvements are likely as further jet calibration tunings, software and analysis algorithm developments are foreseen.

4 Acknowledgments

We thank ARDA-CMS group for the kind help with ASAP job submission tool on the LHC computing grid and C. Weiser for the useful discussions of the CMS b tagging implementation. We are grateful to R. Demina, M. Gruenewald, K. Matchev, J. Mnich, F. Palla and R. Tenchini for the help with the note preparation.

References

[1] F. Abe et al. *Phys. Rev. Lett.*, 71:500, 1993.

[2] F. Abe et al. *Phys. Rev.*, D 50:4252, 1994.

[3] F. Abe et al. *Phys. Rev. Lett.*, 75:1451, 1995.

[4] F. Abe et al. *Phys. Rev.*, D 65:052005, 2002.

[5] F. Abe et al. *Phys. Rev.*, D 66:032002, 2002.

[6] S. Abachi et al. *Phys. Rev. Lett.*, 74:3548, 1995.

[7] B. Abbott et al. *Phys. Lett.*, B 487:264, 2000.

[8] B. Abbott et al. *Phys. Rev. Lett.*, 85:5068, 2000.

[9] C. Adloff et al. *Phys. Lett.*, B 467:156, 1999.

[10] C. Adloff et al. *Erratum Phys. Lett.*, B 518:331, 2001.

[11] C. Breitweg et al. *Eur. Phys. J*, C 18:625, 2001.

[12] A. Aktas et al. *hep-ex/0411046*, 2004.

[13] S. Chekanov et al. *Phys. Rev.*, D 70:012008, 2004.

[14] S. Chekanov et al. *Phys. Lett.*, B 599:173, 2004.

[15] A. Aktas et al. *hep-ex/0502010*, 2005.

[16] M. Acciarri et al. *Phys. Lett.*, B 503:10, 2001.

[17] P. Achard et al. *Phys. Lett.*, B 619:71, 2005.

[18] P. Nason, S. Dawson, and R.K. Ellis. *Nucl. Phys.*, B 303:607, 1988.

[19] P. Nason, S. Dawson, and R.K. Ellis. *Nucl. Phys.*, B 327:49, 1989.

[20] W. Beenakker et al. *Nucl. Phys.*, B 351:507, 1991.

[21] M. Cacciari et al. *JHEP*, 0407:033, and references therein, 2004.

[22] M.L. Mangano. *hep-ph/0411020, and references therein*, 2004.

[23] S. Frixione. *hep-ph/0408317*, 2004.

[24] T. Sjostrand and M. Bengtsson. *Comput. Phys. Comm.*, 43:367, 1987.

[25] S.V. Chekanov. *hep-ph/0211298*, 2002.

[26] A. Heister et al. *CMS Note 2006/036*, 2006.

[27] O. Kodolova. *CMS CR 2005/019*, 2005.

[28] Volume I CMS PTDR. *CERN/LHCC 2006-001*, 2006.

[29] S. Agostinelli et al. *Nucl. Instr. Meth.*, A 506:250, 2003.

[30] ORCA: CMS OO Reconstruction. *http://cmsdoc.cern.ch/orca*.

[31] ASAP. *http://www-asap.cern.ch/e2e/user_guide.php*.

[32] CMS TDR 6.2. *CERN/LHCC 2002-26*, 2002.

[33] M. Vos and F. Palla. *CMS Note 2006/030*, 2006.

[34] S. Esen and R. Harris. *CMS Note 2006/069*, 2006.

[35] S. Eidelman et al. *Phys. Lett.*, B 592:1, 2004.

[36] C. Weiser. *CMS Note 2006/014*, 2006.

	MC input, $120 < \hat{p}_{\mathrm{T}} < 170$ GeV/c	Fit result
$N_{\mathrm{b\bar{b}}}$	2503	2750 ± 346
$N_{\mathrm{c\bar{c}}}$	965	702 ± 513
N_{uds}	299	329 ± 235
	MC input, $230 < \hat{p}_{\mathrm{T}} < 300$ GeV/c	Fit result
$N_{\mathrm{b\bar{b}}}$	5250	5222 ± 501
$N_{\mathrm{c\bar{c}}}$	2388	2050 ± 728
N_{uds}	1740	1778 ± 341
	MC input normalized to 10 fb^{-1} luminosity, million events	Fit result, million events
$N_{\mathrm{b\bar{b}}}$	11.2	10.1 ± 1.6
$N_{\mathrm{c\bar{c}}}$	4.6	5.4 ± 2.0
N_{uds}	1.2	1.3 ± 0.9

Table 1: Results of the fit to the distribution of the transverse momentum of the muon with respect to the nearest b tagged jet. The number of beauty, charm and light quark events in the Monte Carlo input are shown together with the fit result for those event sources.

$\hat{p}_{\mathrm{T}}$, GeV/c	σ^{QCD}, μb	$\mathrm{N}^{\mathrm{QCD}}_{\mathrm{generated}}$, events	$\mathrm{b\bar{b}}$ purity, %	$\mathrm{c\bar{c}}$ fraction, %	uds fraction, %	$\mathrm{N}^{\mathrm{b\bar{b}}}_{\mathrm{expected}}$, events
$50-80$	20.9	198993	66	32	2	1.4 M
$80-120$	3.0	294986	66	32	2	6.1 M
$120-170$	0.5	291982	72	26	2	5.1 M
$170-230$	0.1	355978	71	26	3	2.4 M
$230-300$	2.4×10^{-2}	389978	73	24	3	0.9 M
$300-380$	6.4×10^{-3}	283983	70	25	5	0.3 M
$380-470$	1.9×10^{-3}	191989	68	27	5	88 k
$470-600$	6.9×10^{-4}	190987	64	29	7	34 k
$600-800$	2.0×10^{-4}	94996	60	31	9	10 k
$800-1000$	3.6×10^{-5}	89999	60	30	10	2.0 k
$1000-1400$	1.1×10^{-5}	89998	55	31	14	0.5 k

Table 2: B purity and number of expected events after the final event selection. The expected number of $\mathrm{b\bar{b}}$ events is quoted for 10 fb^{-1} integrated luminosity.

Source	uncertainty, %
jet energy scale	12
event selection	6
B tagging	5
luminosity	5
trigger	3
muon Br	2.6
misalignment	2
muon efficiency	1
$t\bar{t}$ background	0.7
fragmentation	9
total	18

Table 3: Sources of systematic uncertainties on the inclusive b production cross section measurement. The total systematic uncertainty is calculated by adding all contributions in quadrature.

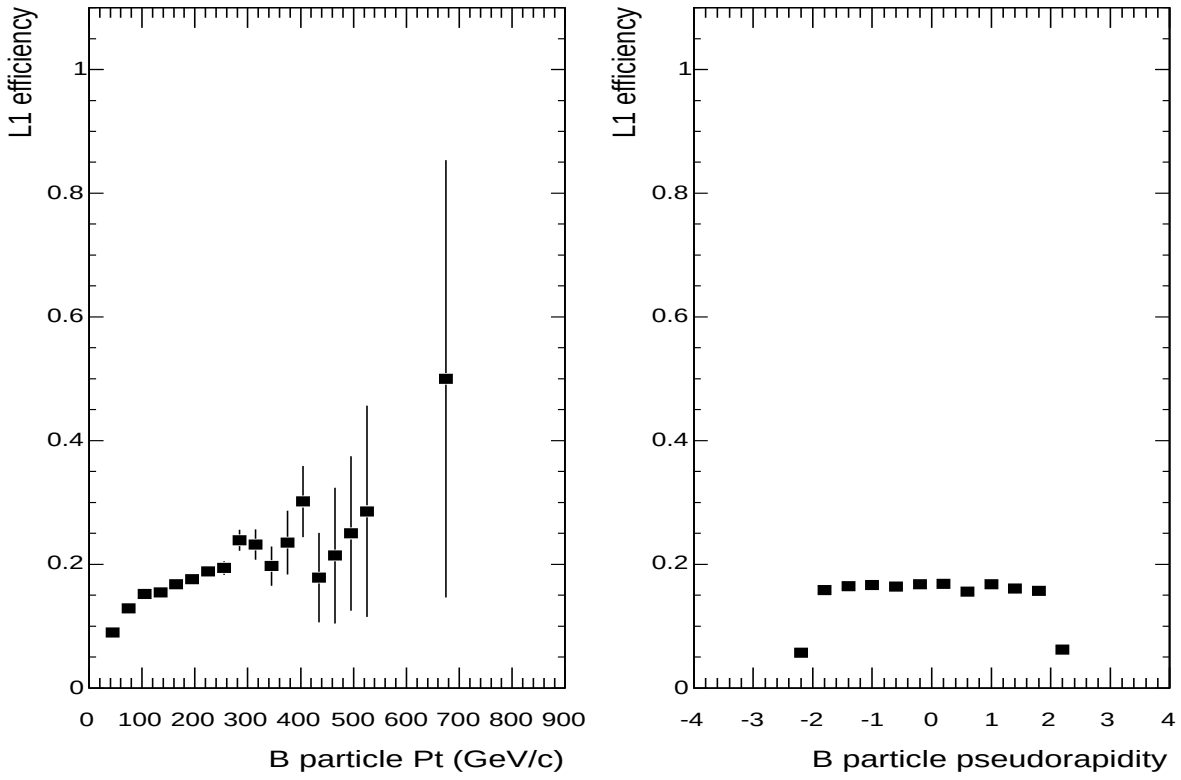

Figure 1: The L1 trigger efficiency for selecting events with B hadrons with $p_{\mathrm{T}} > 50\ \mathrm{GeV}/c$ contained within $|\eta| < 2.4$. The left plot shows the efficiency as a function of the generated B hadron momentum. The right plot shows the efficiency as a function of the generated B hadron η.

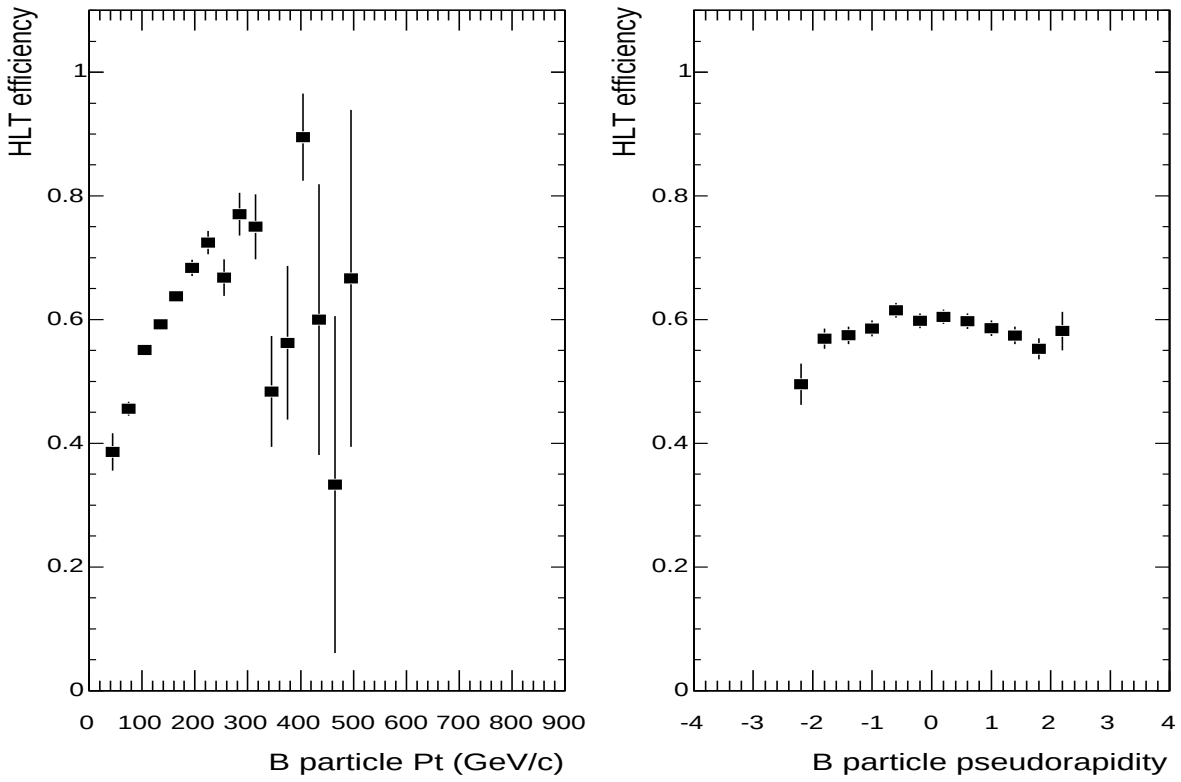

Figure 2: The HLT trigger efficiency for selecting events with B hadrons with $p_{\mathrm{T}} > 50$ GeV$/c$ contained within $|\eta| < 2.4$. The left plot shows the efficiency as a function of the generated B hadron momentum. The right plot shows the efficiency as a function of the generated B hadron η. The HLT efficiency is computed on already L1 selected events.

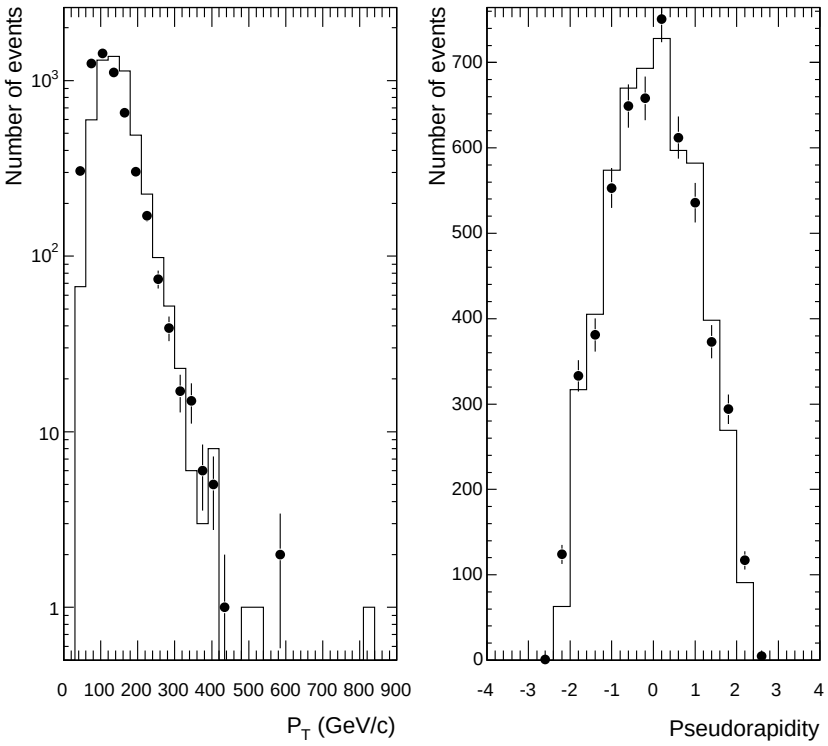

Figure 3: Reconstructed (dots) p_{T} (left plot) and pseudorapidity η (right plot) of the most energetic b tagged jet versus p_{T} and pseudorapidity of the most energetic generated (histograms) B-particle.

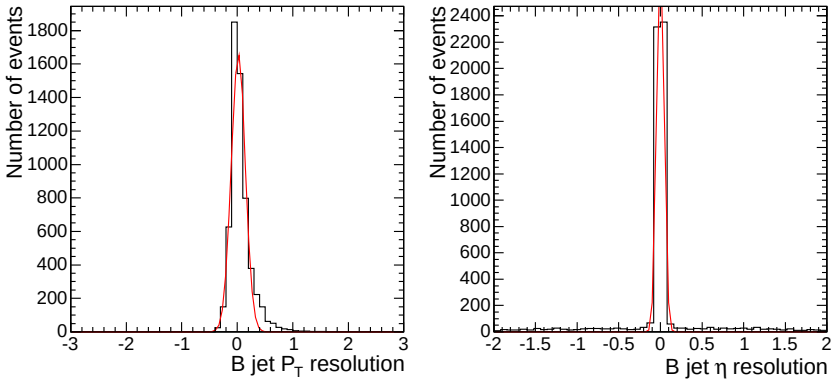

Figure 4: Relative resolution, (Reconstructed $-$ True) / True, for p_{T} and absolute resolution, (Reconstructed $-$ True), for pseudorapidity of b tagged jets in CMS.

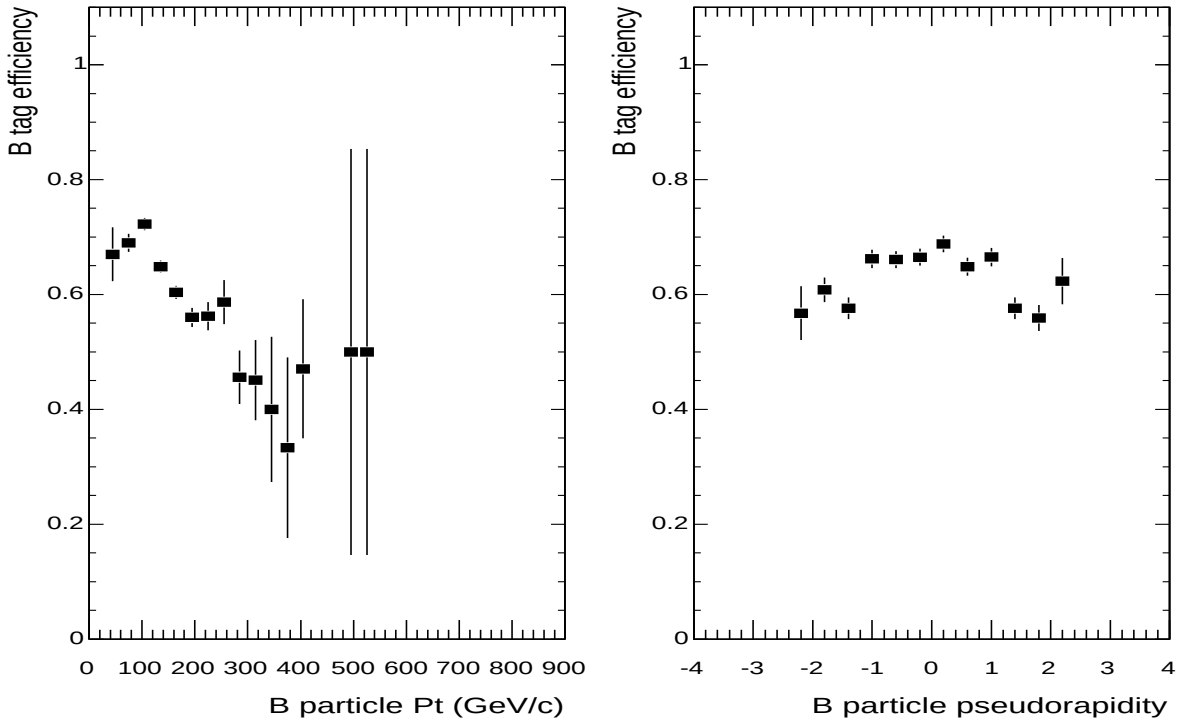

Figure 5: The b tagging efficiency versus p_{T} and pseudorapidity of the generated B-particle. The efficiency is computed on already triggered (both L1 and HLT) events.

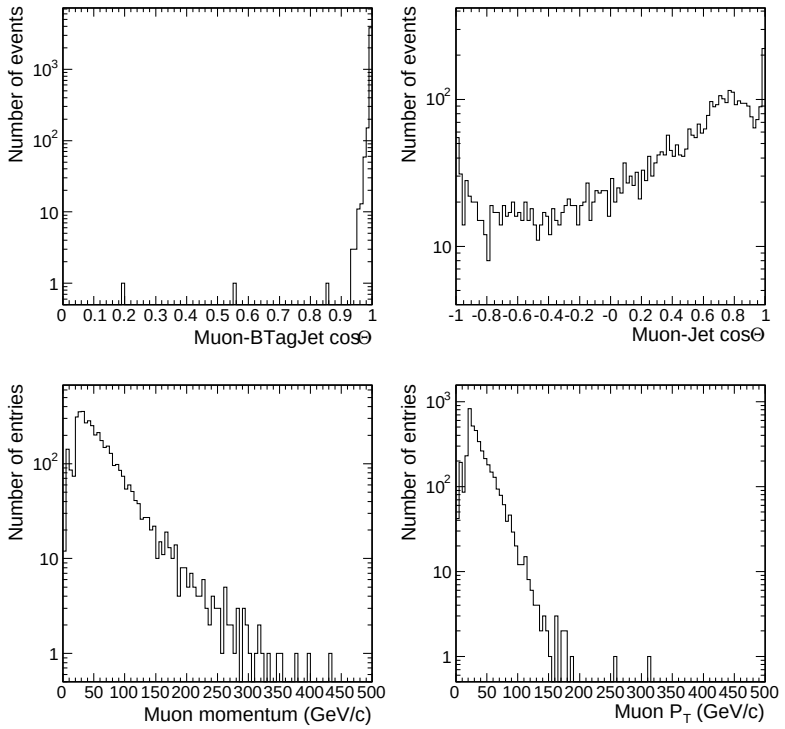

Figure 6: Angular distance between the tagged muon and the b tagged jet (left-top plot), distance between the tagged muon and the second closest jet (right-top plot), muon momentum (left-bottom plot) and muon transverse momentum with respect to the beam line (right-bottom plot) distributions.

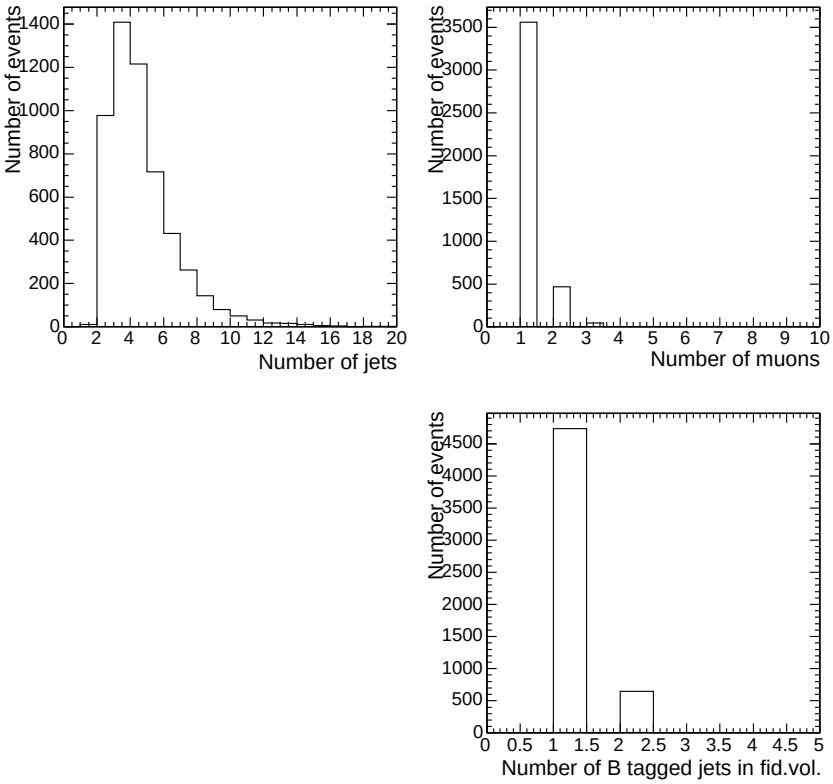

Figure 7: Distributions for the number of jets (left-top plot), number of muons (right-top plot) and number of B tagged jets in the fiducial volume (right-bottom).

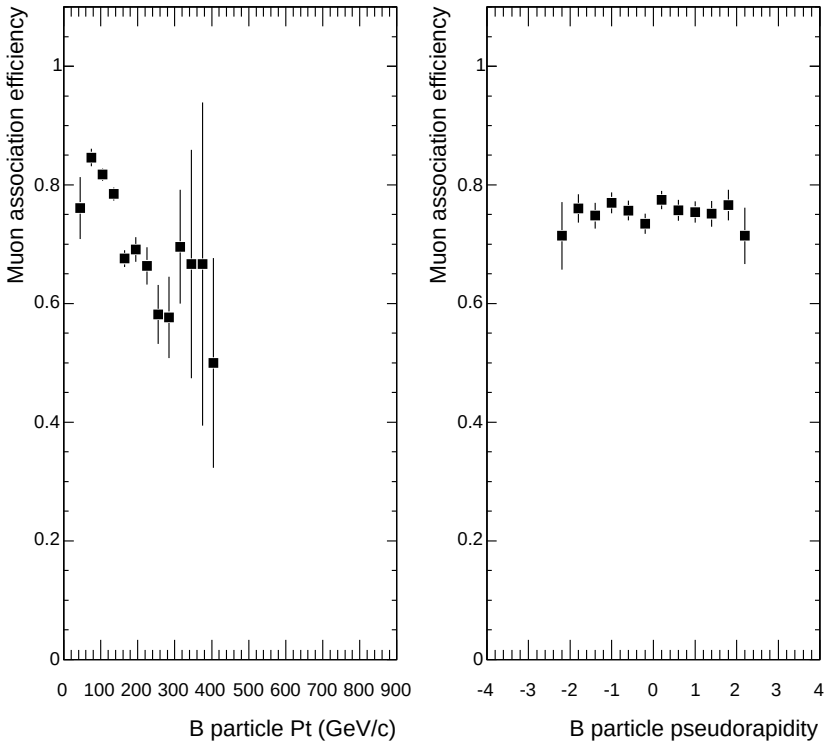

Figure 8: The efficiency of the muon association with b tagged jet.

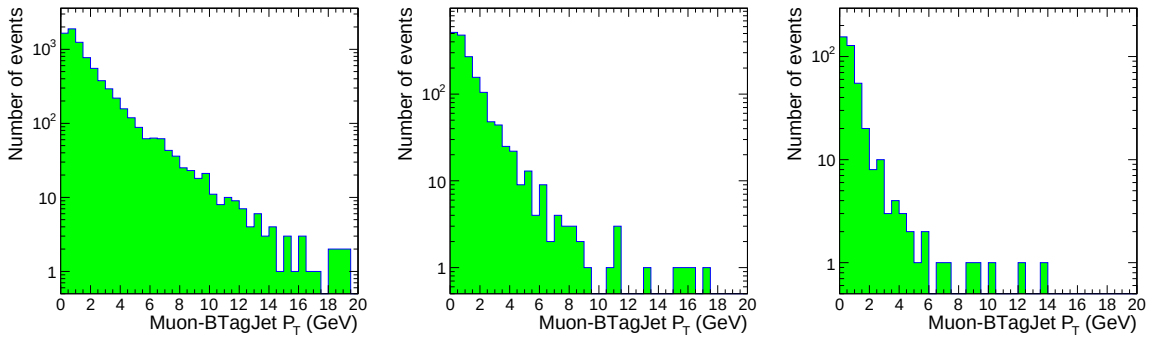

Figure 9: Spectra of p_{T} with respect to the closest b tagged jet of muons detected in the CMS muon spectrometer from three sources: beauty events (left plot), charm events (middle plot) and light quark events (right plot).

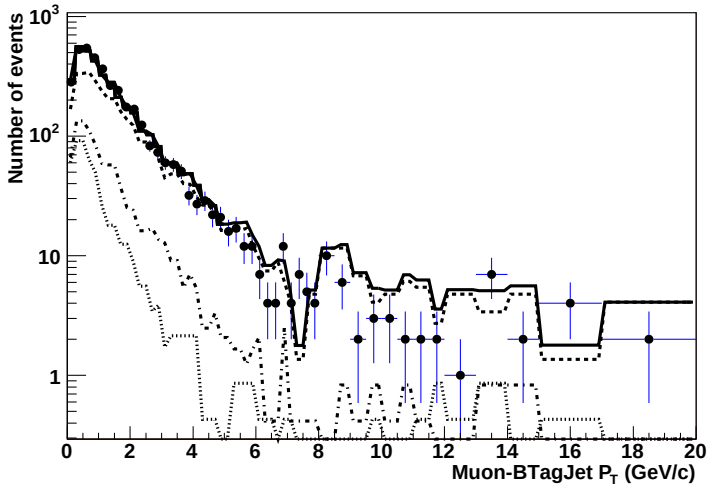

Figure 10: Fit of the muon p_{T} spectrum with respect to the closest b tagged jet. The sample of generated QCD events with "p_{T}-hat" parameter in the range $120 < \hat{p_{\mathrm{T}}} < 170$ GeV$/c$ is tested. The contributions of tagged muons from b events (dashed curve), c events (dot-dashed curve) and light quark events (dotted curve) as defined by the fit are shown. The solid curve is the sum of the three contributions.

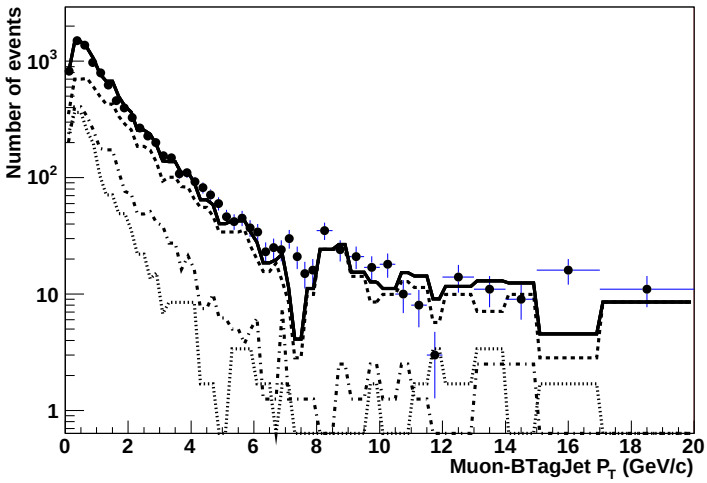

Figure 11: Fit of the muon p_{T} spectrum with respect to the closest b tagged jet. The sample of generated QCD events with "p_{T}-hat" parameter in the range $230 < \hat{p_{\mathrm{T}}} < 300$ GeV/c is tested. The contributions of tagged muons from b events (dashed curve), c events (dot-dashed curve) and light quark events (dotted curve) as defined by the fit are shown. The solid curve is the sum of the three contributions.

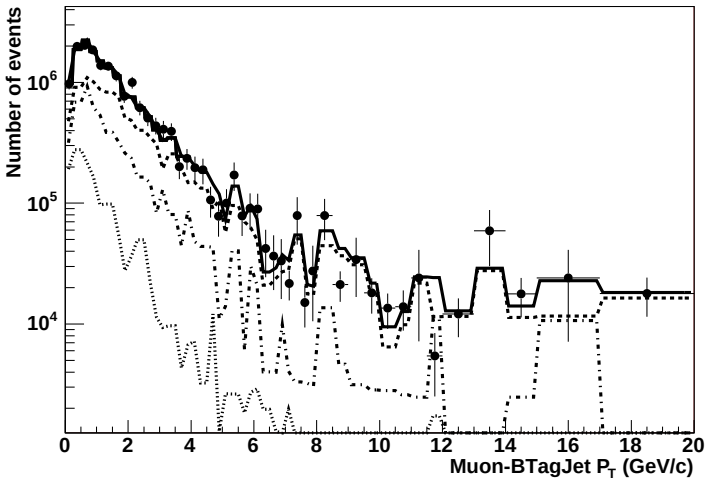

Figure 12: Fit of the muon p_{T} spectrum with respect to the closest b tagged jet. The generated QCD events of all samples with "p_{T}-hat" parameter in the range $\hat{p_{\mathrm{T}}} > 120$ GeV/c are tested. The samples are combined by normalizing to the same integrated luminosity (10 fb^{-1}). The contributions of tagged muons from b events (dashed curve), c events (dot-dashed curve) and light quark events (dotted curve) as defined by the fit are shown. The solid curve is the sum of the three contributions.

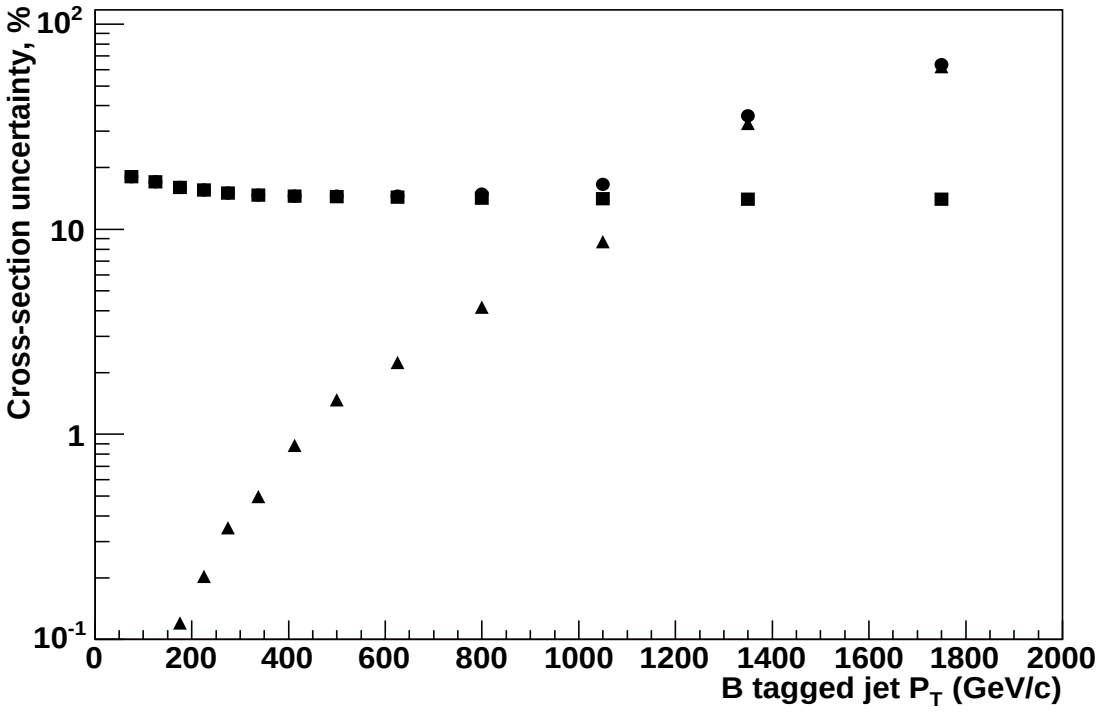

Figure 13: The statistical uncertainty for the cross section measurement (triangles), systematic (squares) uncertainty and total (dots) uncertainty as function of the b tagged jet transverse momentum with respect to the beam line. Total uncertainty comprises the statistical and systematic uncertainties added in quadrature.